1. Kasa Sudheer[1], 2. Penagaluru Suresh[1] 3. R Sireesha[1] 4. K Yamuna[1]

Department of EEE, Sri Venkateswara College of Engineering, Tirupati, India.

doi:10.15199/48.2024.06.22

COVID-19 Propagation Unified Controller for Improved Power Quality in Multi Feeder Renewable Integrated System

Abstract. *Modern power system topologies have undergone significant alterations as a result of advancing technology. Most improvements in topologies of power system have been implemented to ensure a consistent power delivery and to meet the growing global demand for energy. This research examines a specialized two-line source system. Power quality problems on both lines have been examined with the help of Multi Converter Controller. To effectively reduce harmonics, a modified COVID-19 Propagation based DQ current controller for shunt converters and an ANFIS-based DQ controller for series converters are proposed here. Proposed COVID-19 Propagation Unified (CPU) Controller effectually alleviates anomalous in voltage and current. Performance of CPU Control technique is compared with soft computing techniques in MATLAB/SIMULINK.*

Streszczenie. *Topologie współczesnych systemów elektroenergetycznych uległy znaczącym zmianom w wyniku postępu technologicznego. Większość ulepszeń w topologii systemu elektroenergetycznego została wdrożona w celu zapewnienia spójnego dostarczania mocy i zaspokojenia rosnącego światowego zapotrzebowania na energię. W badaniu tym analizowany jest wyspecjalizowany dwuliniowy system źródłowy. Problemy z jakością energii na obu liniach zostały zbadane za pomocą kontrolera Multi Converter. Aby skutecznie zredukować harmoniczne, zaproponowano tutaj zmodyfikowany sterownik prądu DQ oparty na propagacji COVID-19 dla przetwornic bocznikowych i sterownik DQ oparty na ANFIS dla przetwornic szeregowych. Proponowany ujednolicony kontroler propagacji wirusa COVID-19 (CPU) skutecznie łagodzi anomalie w napięciu i prądzie. Wydajność techniki CPU Control porównano z technikami miękkiego przetwarzania w MATLAB/SIMULINK (**Ujednolicony kontroler propagacji wirusa COVID-19 zapewniający lepszą jakość energii w zintegrowanym systemie wielopodajnikowym odnawialnych źródeł energii**)*

Keywords: Renewable Sources, PI, ANFIS Controller, COVID-19 Propagation Algorithm, Power Quality, **UPQC.**
Słowa kluczowe: Źródła odnawialne, PI, kontroler ANFIS, algorytm propagacji COVID-19, jakość energii, UPQC

Introduction

The grid is being injected with alternative energy sources as a result of growing worries about global warming and the need to deliver power to dramatically shifting load demand. Degraded power quality is brought on by the addition of renewable sources and drastically shifting nonlinear loads [1-2]. Power quality must be raised in order to deliver a stable supply [3].

Numerous studies in earlier studies have suggested various controllers for reducing problems with power quality. Examples are Shunt Controllers [4] to alleviate current irregularities, Dynamic Voltage Restorers to suppress voltage disturbances [5], and Unified Power Quality controllers to eliminate current, voltage, and harmonics. Unified Power Quality controllers have dominating traits in comparison with other methods that have been demonstrated to improve overall system effectiveness [6]. Performance is increased by properly integrating renewable energy sources with the aforementioned controllers. The effectiveness of controllers in correcting power quality concerns is aided by the use of unified power quality controller [7], dynamic voltage restorer [5], and renewable integrated shunt controller [4]. Interline and generalized unified power flow controllers have been discussed in multi-line power system. Connecting various loads to power system becomes more complex every day. Power quality problems on multi lines are handled simultaneously by Multi Converter Controllers [7].

For improved performance in dealing with power quality issues efficient mitigating techniques are needed. Bang-bang method [8], p-q theory [9], D-Q theory, modified D-Q method [10], and I cosine technique [7] are just a few of the controlling algorithms that have been proposed for shunt controllers. For series controller, DQ controller and power angle controller were suggested. Combining these controlling algorithms suggested the use of unified power quality controllers to reduce both voltage and current defects.

Traditional PI controllers are being replaced by soft computing techniques with more robust properties, such as fuzzy controllers [11], ANN controllers [4], Bio Inspire swarm optimization method [12] & Genetic Algorithm [13]. Here, COVID-19 Propagation [14] based modified DQ control algorithm for shunt controller (ShC) & ANFIS-based DQ theory to series controllers (SeC) employed to enhance total performance of considered multi feeder system. The proposed model primarily focuses on reducing voltage abrupt conditions like harmonics in V & I, Sag and swell in Voltage, and interruption, in addition to that integrating renewable sources and compensating for imbalanced voltages.

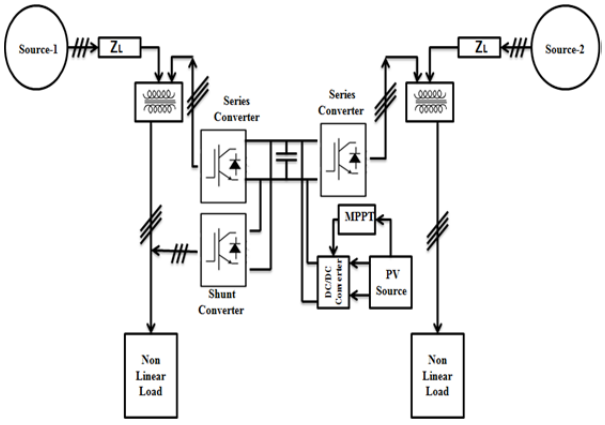

Fig.1. Proposed Multi Feeder System model

Multi Feeder System Description

Proposed Multi Feeder system is depicted in Fig. 1. Two parallel lines supplying various loads are connected with a renewable source integrated Unified Current Controller (UCC). The model under consideration has two separate loads, L1 and L2, are supplied by sources S1 and S2. S1 is coupled to Non-Linear type of Load (L1), served by S1, and Source-2 serves Sensitive type of Load. The Supply voltages are V_{S1} & V_{S2}, the supply currents are I_{S1} and I_{S2}, and load currents are I_{L1} & I_{L2}. Here three voltage source inverters utilized in the proposed UCC. Two inverters are tied in series to lines 1 and 2 via injection transformers, acting as series converters (SeC_1 & SeC_2), while remaining

one is tied in shunt to serve as a shunt converter (ShC). Three converters in total share a single DC link. To retain stable voltage at the DC link, a photovoltaic source is integrated to supply required power.

Photo Voltaic Source

For the purpose of reducing current irregularities on Line-1 and providing power to SeC1 and SeC2 during voltage sag, swell, and interruption conditions, a parallel DC link fed PV unit is used. Typically, Lead Acid Batteries, Flywheels, and Ultra Capacitors were used to provide the necessary power at the DC connection [15]. Photo Voltaic Source has replaced the battery in the current model. This provides a portion of real power to load, while acting as voltage stabilizer in DC link. It is depicted in Fig.2.

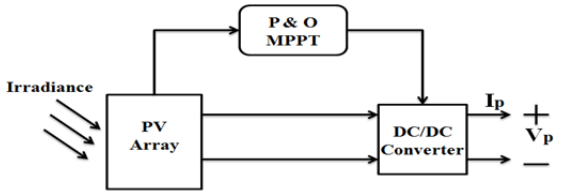

Fig. 2. PV Unit

For tracking the greatest solar energy, a number of MPPT methods were available. Such as soft computing tuned MPPT techniques, incremental conductance, P&O, etc. P&O is the most familiar algorithm for its simplicity, fewer parameters, and straightforward feedback. PV cells, MPPT units, and DC/DC boost converters are included in what is considered a photovoltaic source.

PV source produced power is calculated by Eqn. (1),

$$P_p = V_p * I_p \quad (1)$$

Voltage and Current of PV unit are presented in Eqn.(2) & (3),

$$V_p = \frac{AkT}{q}\log\{\frac{I_{sc}}{I_p} + 1\} \quad (2)$$

$$I_p = I_{sc} - I_{sat}\exp\{\frac{q}{AkT}(V_p + \{I_p R_{se}\}) - 1\} - \frac{V_p + I_{sc}R_{se}}{R_{sh}} \quad (3)$$

DC-DC converter fed with MPPT-controlled PV unit is depicted in Fig. 2. This combination keeps the inverter's DC link voltage constant.

Control Strategy

Modified DQ based control algorithms were suggested for the proposed system consists of both series & shunt controllers. Reference currents are produced using the COVID-19 Propagation - based DQ control algorithm in the shunt controller. Pulse creation from the difference between real and reference currents uses a hysteresis controller. Reference voltage is produced by an ANFIS- DQ controller in a series controller.

Source Controller

Controlled Voltage Source is taken into consideration in the multi feeder system to analyse performance of the Stated SeC & ShC controllers. The modelled control source is shown in Fig.4. Six distinct sinusoidal signal waves are created and combined to provide the desired sinusoidal voltage. The resultant 3 ϕ voltages are presented in Eqn. (4), (5) & (6)

$$S_a = V_{rms}[\sin_1 + (\sin_6 * T_1)] * T_2 \quad (4)$$

$$S_b = V_{rms}[\sin_3 + (\sin_4 * T_1)] * T_2 \quad (5)$$

$$S_c = V_{rms}[\sin_5 + (\sin_2 * T_1)] * T_2 \quad (6)$$

Here, Vrms is the RMS voltage, S_a, S_b, and S_c are 3 ϕ regulated supply voltages, and T1 and T2 are timers that regulate voltage to a predetermined period of time. Controlled voltage source for the suggested system is shown in Fig. 4.

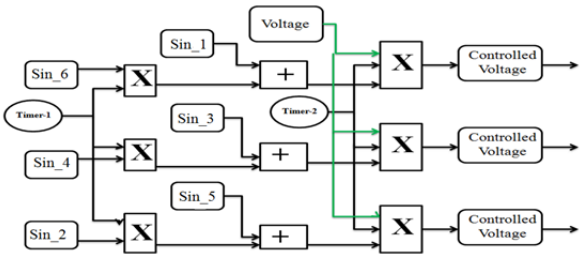

Fig. 3. Controlled Voltage Source

Shunt controller (ShC)

On line-1, Shunt controller (ShC) is fed. It offsets the demand for reactive power. The shunt controller in this instance compensates harmonics and reactive component of Load Current (L1). ShC controls voltage across the DC link as well. The suggested shunt control approach is shown in Fig. 5. In this case, load currents were converted to dq0 components provided by,

$$I_{Ldq0} = T_s * I_{Labc} \quad (7)$$

Here, Ts is transformation matrix

$$T_s = \frac{2}{3}\begin{bmatrix} \mathrm{Cos}[\theta] & \mathrm{Cos}[\theta - 120] & \mathrm{Cos}[\theta + 120] \\ -\mathrm{Sin}[\theta] & -\mathrm{Sin}[\theta - 120] & -\mathrm{Sin}[\theta + 120] \\ 1/2 & 1/2 & 1/2 \end{bmatrix} \quad (8)$$

The dc component of Id is extracted using a low pass filter. In order to stabilize dc link voltage, response of the PI controller is aided with direct axis component of IL. Reference current's d and q components are thus given by

$$I_{ref}^{d} = I_{Ld} + \Delta I_{dc} \quad (9)$$

$$I_{ref}^{q} = I_{Lq} \quad (10)$$

Once more, the reference currents' dq0 components are converted into an ABC component frame using

$$I_{ref}^{abc} = T_s^{-1} * I_{ref}^{dq0} \quad (11)$$

For alleviating reactive power & harmonic components in source current, controller gate pulses are produced using hysteresis.

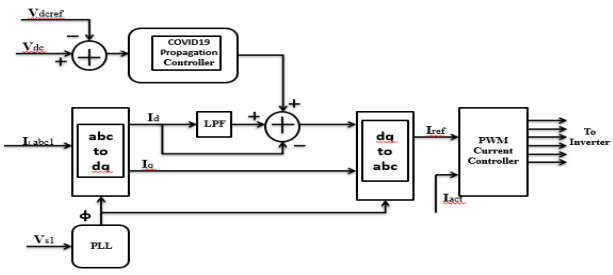

Fig 4. Shunt control with COVID-19 Propagation

The COVID-19 Propagation technique is utilized to calculate the PI controller gain values in this model. This approach replaces the conventional PI controller methodology.

COVID-19 Propagation Technique

Typically imitating natural behaviours, bioinspired models [16] are renowned for their effective use in hybrid approaches to identify parameters for optimization.

In order to locate suboptimal solutions in tolerable execution times, metaheuristics should cope with enormous search spaces, often even infinite ones for continuous cases. The unique metaheuristic called Coronavirus propagation Algorithm, which is proposed in this study, was inspired by the coronavirus's rapid spread and ability to infect the majority of nations in the globe admirably quickly. Major advantages of COVID-19 Propagation [17] Algorithm are

1. It is parametrized with real rates and probabilities, allowing the user to conduct more research without having to do so.
2. Without the requirement for configuration, it can halt the solution investigation after multiple repetitions.

COVID-19 Propagation Algorithm:

Step 1: Create the patient-zero (PZ) initial population.

Step 2: Propagation of Disease. A few of the sick people pass away. As per coronavirus death rate (P_DIE), they pass away. The coronavirus will spread to new people through the survivors (P SUPERSPREADER).

- Common spreaders. SPREADING_RATE

-Super-spreaders. "SUPERSPREADING RATE."

-There is a likelihood that people will travel (P_TRAVEL).

-Individuals have a chance of moving about (P TRAV EL), which makes it possible to spread the disease to potentially very various solutions (TRAV ELER RATE). New solutions will vary at an ORDINARY RATE if you are not a traveller. Keep in mind that one person can be a super-spreader and a traveller.

Step 3: Update population data.

-Dead population. If anybody passes away, their death is added to this population and is permanently lost.

-The population recovery. Following each iteration, sick people are distributed to the population that has recovered after spreading the coronavirus in accordance with the prior stage. If a member of this population meets the requirements for reinfection (P_REINFECTION), they may become infected again at any iteration. An isolated person is deemed to have been sent to recovered population (P_ISOLATION).

- A new infected population. All sick people from each iteration are collected in this population.

Step 4: Apply the stop criteria. The stop criterion may be extended to include a predetermined amount of iterations (PANDEMIC DURATION). Reaching the halt threshold also depends on the social isolation measures.

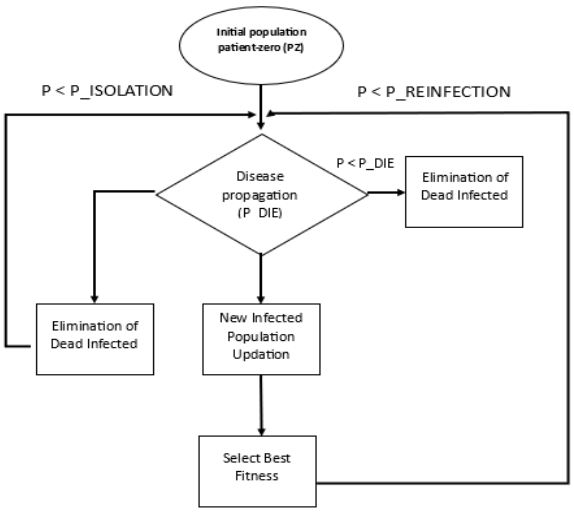

Fig. 5. Flow chart of COVID-19 Propagation Algorithm

Table 1. COVID-19 Propagation values

Parameter	Value
P_DIE	0.06
P SUPERSPREADER	0.1
ORDINARY RATE	3
SUPERSPREADER RATE.	20
P_REINFECTION	0.15
P_ISOLATION	0.5
P_TRAVEL	0.1
PANDEMIC DURATION	30

Series Control Strategy

Here, the function of the series SeC is to reduce voltage sag, swell, and interruption. Additionally, it corrects harmonics in voltage. Fig. 7 depicts the proposed series voltage controller. Source voltages were first converted into a synchronous dq0 reference frame by employing,

$$(12)\quad V_{s1}^{dq0} = T_s * V_{s1}^{abc} = V_{s1p} + V_{s1n} + V_{s10} + V_{s1h}$$

where, respectively, V_{s1p}, V_{s1n}, V_{s10}, and V_{s1h} stand for positive, negative, zero-order, and harmonic components.

To obtain sinusoidal voltages, dq0 reference components of load voltage given by

$$(13)\quad V_{L1}^{dq0} = T_s * V_{s1}^{abc} = \begin{bmatrix} U_m \\ 0 \\ 0 \end{bmatrix}$$

The dq0 reference frame compensating voltage is,

$$(14)\quad V_{dq0}^{ref} = V_{s1}^{dq0} - V_{L1}^{dq0}$$

The compensatory voltage in turn converted to the ABC frame. The gate triggering pulses are produced using SPWM for compensating deviation in load voltage.

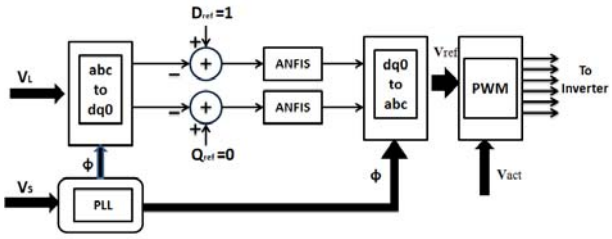

Fig. 7. Series Controller

Nuero-Fuzzy Controller

The Nuero- Fuzzy (ANFIS) controller makes use of both fuzzy inference and the adaptive learning capabilities of neural networks. In [8,12], the neuro-fuzzy combination has demonstrated its ability to fine-tune error signals. The present model, depicted in Figure 8, has a five-layer ANFIS structure, and Figure 9 depicts the sugeno rules that the ANFIS controller employs.

Primary layer response:

$$(15)\quad Z_1 = \mu f(e_1)$$

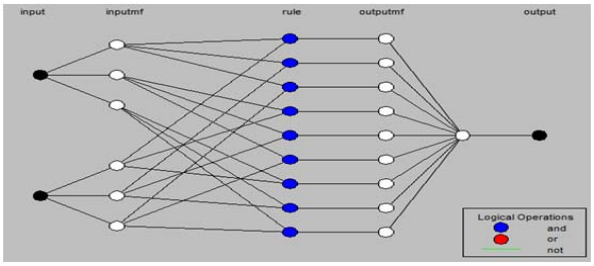

Fig. 8. Structure of ANFIS Controller

Secondary layer: performs inputs multiplication as shown in (2.21). It possesses fixed nodes.

$$(16)\quad Z_2 = \mu_{fi}\, f(e_1)\, \mu_{gi} f\,(e_2)$$

Here, e_1 & e_2 = Error & Change in Error

Tertiary layer: each node performs ratio of ith firing to net firing strengths, It possesses fixed nodes.

$$Z_3 = W_i' = \frac{W_i}{W_1 + W_2} \quad (17)$$

Fourth layer: these were adaptive nodes in nature & it performs,

$$Z_4 = W_i' (p_i e_i + Q_i e_2 + R_i) \quad (18)$$

Fifth layer: It has fixed nodes, performs amalgamation of all the inputs to derive final response,

$$Z_5 = \sum(Z_{4i}) \quad (19)$$

The above result is identical to that of the Fuzzy System used in [20]. Here, learning about ANFIS is a two-way process. For forward learning procedure, LSE method is employed. Back propagation learning is used in reverse direction. Three linguistic fuzzy values (Low, Medium, and High) are chosen, for a single output and two input variables in the current ANFIS model.

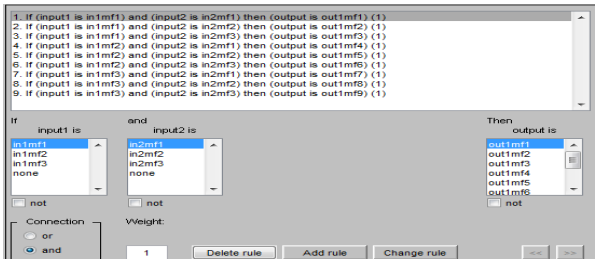

Fig. 9. Rules used in ANFIS controller

Table 2. Proposed System Specifications

Parameters	Ratings
Source voltage	3-phase 380 V, 50 Hz
Source impedance	R_S = 0.1ohm, L_S = 0.001mH
Solar Cell	35 V & 6 A
Load-1	R = 16.66 ohm L = 30 mH
DC link	V_{dc} = 600 V
Load-2	R =10 ohm , L = 0.03 mH

Results & Discussion

Current Profile

Harmonics are inoculated by nonlinear loads linked to Line-1. The COVID-19 Propagation based ShC injected currents (Phase-A) for suppressing harmonics in supply current are presented in Fig. 10. Nonlinearities exist in the supply current before t = 0.1 seconds. The COVID-19 Propagation based shunt controller becomes active at time t = 0.1 seconds and suppresses nonlinearities by injecting the opposite current. In this instance, both Source and PV-fed ShC injected current serves the load.

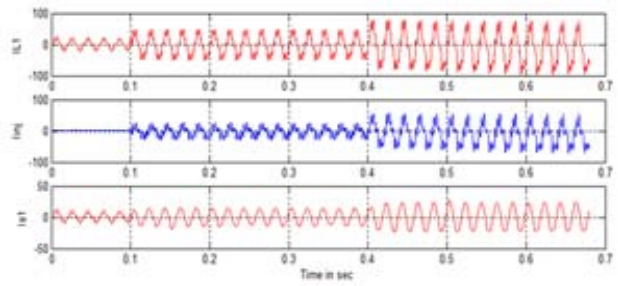

Fig. 10. Load (L1), Injected and Source (S-1) Currents on Line-1

Voltage Disturbance Mitigation

The voltage on Line-1 experiences a 25% sag between 0.15 and 0.25 sec and a 20% swell between 0.35 and 0.5 sec. to correct the sag and swell in the voltage of Load-1, the Series Voltage Controller (SeC-1) injects voltage. The same is depicted in Fig. 11.

Line-2 voltage exhibits a 25% sag between 0.15 and 0.25 sec and a 30% swell between 0.3 and 0.4 sec. With a three-phase fault, a voltage drop occurs between 0.45 and 0.55 sec. To correct sag, swell, and interruption, the series voltage controller (SeC-2) injects voltage. The same is depicted in Fig. 12.

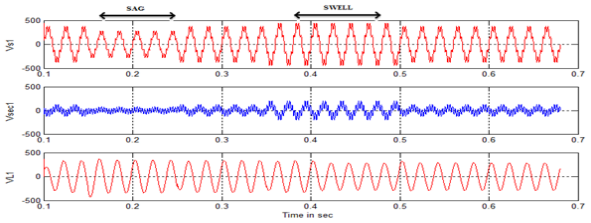

Fig. 11. Source-1 Voltage, Injected Voltage and Load-1 Voltage on Line-1

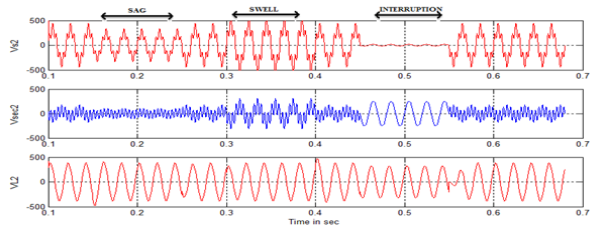

Fig. 12. Source, injected & Load-2 voltage on Line-2

The distorted and imbalanced voltage on Line-1 is shown in Fig. 13. In this case, distorted unbalanced voltages created between t = 0.1 sec and t = 0.2 sec. Similarly, between t = 0.2 sec and 0.3 sec unbalanced sinusoidal voltages are produced. In order to suppress the irregularities, Sec-1 injects compensating voltages. The delivery of sinusoidal balanced voltages to Load-1 is made possible by the injection of compensating voltage.

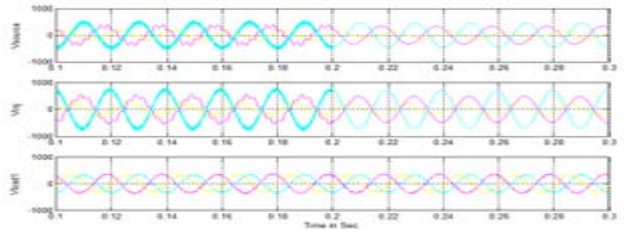

Fig. 13. Compensation of impabalance voltages

Power Supply

Real and reactive power transferred to the load from the source and the photovoltaic unit fed shunt controller are shown in Fig. 14. Real power for Load-1 is provided by Photovoltaic Unit & Source-1. Post t= 0.1 sec, as desired reactive power is injected by the shunt converter, reactive power from the source is lowered. Post t = 0.1 sec, Fig.15 depicts the power factor improvement with shunt controller integration.

Table 3. Comparison of %THD & pf with PI & COVID-19 propagation based-pi controller

Parameters	Without UCC	With PI -UCC	With COVID19 based UCC
P F	0.68	0.91	0.98
%THD			
Source current	26.76	7.77	2.12

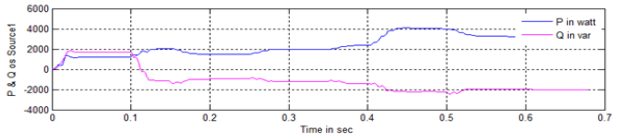

14(a)

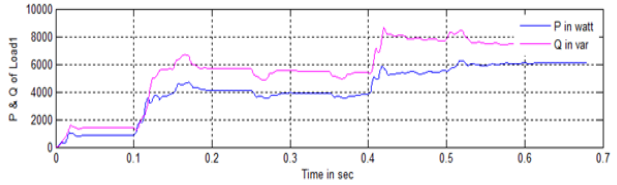

14(b)

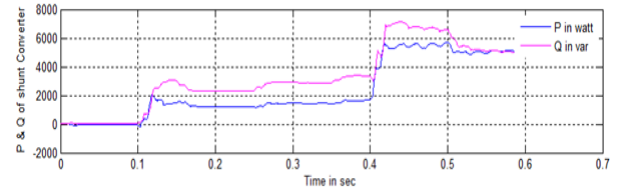

14(c)

Fig. 14. Source-1, Load-1 and Shunt converter Real and reactive power.

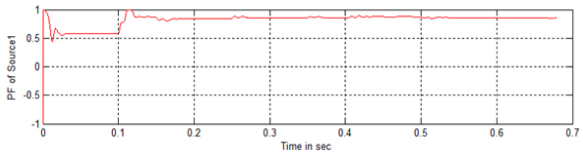

Figu. 15 Improvement of Power Factor on Line-1

Different scenarios are examined for harmonic suppression. such as PI-UCC, COVID-19 Propagation - UCC, and UCC without a controller.

Case 1: Fig. 16 displays the source current % THD Without controller. Due to the existence of harmonic components brought on by nonlinear loads, supply current (Phase-A) THD is greater than average.

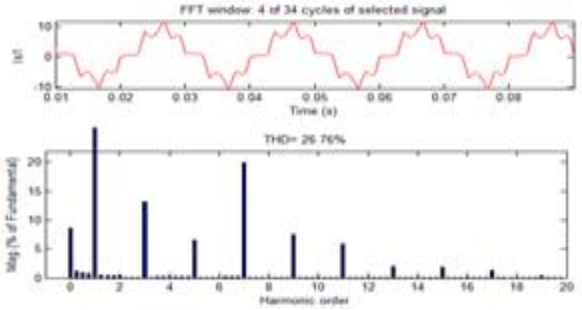

Fig. 16. Source-1 current % THD without UCC & with PI-UCC

Case 2: At t = 0.1 seconds, the proposed UCC is activated. Fig.17 shows that when the PI based UCC is activated, the source current % THD is decreased to 7.7%.

Case 3: In this instance, the PI controller is changed to a COVID-19 Propagation based controller. %THD is decreased to 2.12% with COVID-19 Propagation -based UCC controller, shown in Fig. 18.

Voltage across Load-1 was reduced by % THD, with ANFIS based SeC controller, which is shown in Fig. 19. It is evident from Table 3 that the COVID-19 Propagation - based UCC outperforms than the conventional PI controller in cutting down on source current harmonics.

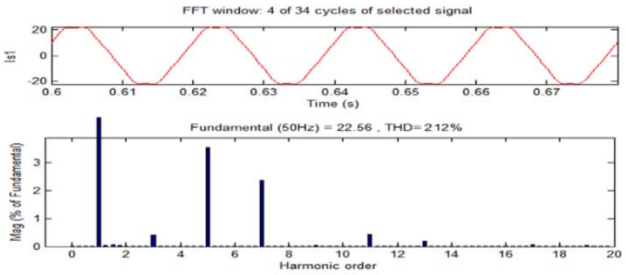

Fig.17. When the PI based UCC is activated, the source current % THD is decreased to 7.7%

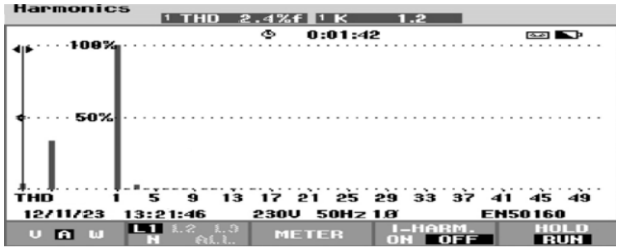

Fig. 18. Source-1 current % THD with COVID-19 Propagation based UCC simulation & Experimental value

Table 3 compares the reduction of current harmonics on Line-1. The COVID-19 Propagation - based shunt controller in the table achieves %THD within standards. Additionally, an ANFIS tuned series controller achieves voltage with %THD within predetermined norms.

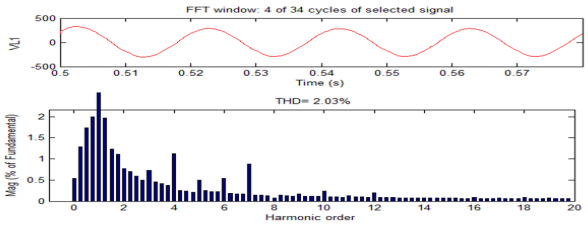

Fig. 19 Load-1 voltage % THD with UCC

Conclusion

Current and voltage harmonics as well as the need for reactive power are successfully compensated by the proposed COVID-19 Propagation Based Unified Multi Converter Controller. It also demonstrates how power is effectively shared between two lines. The model reduces voltage disruptions like interruption, sag, and swell. When compared to the conventional PI-based controller, the COVID-19 Propagation -based controller exhibits superior current harmonic reduction. The model succeeds in achieving effective power quality with renewable integration.

Authors/ *Kasa Sudheer, Email: sudheer.kasa@gmail.com Penagaluru Suresh Email: suresh.penagaluru@gmail.com, R Sireesha, Email: sireesha253@gmail.com & K Yamuna Email: yamunakrishnareddy@gmail.com. Address: Dept. of EEE, Sri Venkateswara College of Engineering, Tirupati, India - 517507.*

REFERENCES

[1] Cherfi, Mohamed Khelil, Abderrezak Gacemi, Abdelkader Morsli, and Abdelhalim Tlemçani. "Compensation of harmonics using a shunt active power filter powered by a photovoltaic source." Przeglad Elektrotechniczny 99, no. 6 (2023).

[2] Seme, Sebastijan, Bojan Štumberger, Miralem Hadžiselimović, and Klemen Sredenšek. "Solar photovoltaic tracking systems for electricity generation: A review." Energies 13, no. 16 (2020): 4224.

[3] Benysek, Grzegorz, and Marian Pasko. Power theories for improved power quality. Heidelberg: springer, 2012.
[4] Ramasamy, Sudha, and K Sudheer. "Enhancement of power quality in renewable source integrated three phase system with ICC controller." Journal of Green Engineering 8, no. 1 (2018): 71-88.
[5] Ramasamy, M., and S. Thangavel. "Photovoltaic based dynamic voltage restorer with power saver capability using PI controller." International Journal of Electrical Power & Energy Systems 36, no. 1 (2012): 51-59.
[6] Reisi, Ali Reza, Mohammad H. Moradi, and Hemen Showkati. "Combined photovoltaic and unified power quality controller to improve power quality." Solar Energy 88 (2013): 154-162.
[7] Sudheer, K., & Sudha, R. Enhancement of power quality in multi feeder three phase system with photovoltaic fed ANFIS-unified multi converter controller. In MATEC web of conferences (Vol. 225, p. 03015).(2018) EDP Sciences.
[8] Kasa, S., & Ramasamy, S. Mitigation of current harmonics in renewable source integrated grid topology with fuzzy based dynamic shunt active filter. In 2017 Innovations in Power and Advanced Computing Technologies (i-PACT) (pp. 1-6)(2017). IEEE.
[9] Montero, Mara Isabel Milans, Enrique Romero Cadaval, and Fermn Barrero Gonzalez. "Comparison of control strategies for shunt active power filters in three-phase four-wire systems." IEEE transactions on power electronics 22, no. 1 (2007): 229-236.
[10] Suresh, P., & Manohar, T. G. (2018). Effective Renewable Source Integration using Unified Power Quality Conditioner with Power Quality Enhancement in Three Phase System. In MATEC Web of Conferences (Vol. 225, p. 05014). EDP Sciences.
[11] Bessadet, Ibtissam, and Hamza Tedjini. "Implementation of a cascaded fuzzy sliding mode control of hybrid power filter." Przeglad Elektrotechniczny 99, no. 6 (2023)
[12] Sarker, Krishna, Debashis Chatterjee, and S. K. Goswami. "Grid integration of photovoltaic and wind based hybrid distributed generation system with low harmonic injection and power quality improvement using biogeography-based optimization." Renewable Energy Focus 22 (2017): 38-56.
[13] Kumar, Parmod, and Alka Mahajan. "Soft computing techniques for the control of an active power filter." IEEE transactions on power delivery 24, no. 1 (2008): 452-461.
[14] Martínez-Álvarez, Francisco, Gualberto Asencio-Cortés, José F. Torres, David Gutiérrez-Avilés, Laura Melgar-García, Rubén Pérez-Chacón, Cristina Rubio-Escudero, José C. Riquelme, and Alicia Troncoso. "Coronavirus optimization algorithm: a bioinspired metaheuristic based on the COVID-19 propagation model."
Big data 8, no. 4 (2020): 308-322.
[15] Penagaluru, S., & Manohar, T. G. (2018). Review on renewable source integrated topologies with power quality enhancing strategies. International Journal of Renewable Energy Research, 8(4), 2350-2366.
[16] Logeswaran, T., and A. Senthilkumar. "Grid connected photovoltaic systems power quality improvement using adaptive control strategy." International journal of Bio-inspired computation 10, no. 3 (2017): 188-204.
[17] El Majdoubi, Omayma, Farah Abdoun, and Otman Abdoun. "An improved approach to resolve a combinatorial optimization problem based Corona Virus Optimization Algorithm." In E3S Web of Conferences, vol. 351, p. 01025. EDP Sciences, 2022.